

Semi-Automatic Enhancement of Atrial Models to Include Atrial Architecture and Patient Specific Data: For Biophysical Simulations

BD Flores Hermosillo

University of Hull, Hull, UK

Abstract

Despite its large influence on biophysical simulations, the underlying anatomical representation is often oversimplified.

The need for more detailed anatomical models has been identified by numerous authors [1-3]. An atrial model including macro and microscopic muscle architecture would help improve the correlation between real and virtual ECGs. In addition it provides a mean to de-couple the simulation domains (anatomy and physiology).

A tool developed to create such models is presented. It readily allows fine-tuning factors such as: connectivity, discontinuity, fiber orientation, muscle architecture, and heterogeneities. The algorithms that speed up the conversion of a 3D heart mesh in raw format, into a detailed model of the atria are explained.

As a result, patient-specific models are brought one step closer.

1. Introduction

The idea of patient-specific simulations of the electric activity of the atria (or the heart as a whole) is in itself tantalizing. Unfortunately, there are still a number of unfulfilled pre-requisites; to name a few: detailed anatomical models, clinical imaging data for validation and faster construction of these (i.e. human atrial DTMRI), mathematical models of specialized structures (work in progress, see [4] and [5]), better approximations for the Inverse Solution (mapping body surface potentials to epicardial potentials).

The work presented here aims to provide the required anatomical representation and to facilitate the construction of patient-specific anatomical models by means of a base model and patient-specific imaging data.

2. Methods

The initial input is a mesh representing the atria, made up of regular elements (e.g. tetra or hexahedrons). Ideally

this would have been obtained from either MRI or CT volumetric data. The mesh can be structured or unstructured, adaptive or not.

There are two facets of the modeling process: (A) Creating base models which will serve as “best template” fitting into new input meshes & (B) Semi-automatically enhancing new meshes using the base models.

A number of base models would be required; a base model of the heart of an adult male is not likely to be best fit for a young female’s heart mesh.

In both scenarios, an electric grid is embedded in the mesh as follows: each *geometric element* (polyhedron) represents from the anatomical point of view, a *myocyte aggregate* which can have a fiber orientation. For biophysical modeling, it represents a single myocyte, the *basic simulation element* for the mathematical approximations of electric activity in the heart; a grid node is placed in the centroid of each element. Full connectivity by gap junctions to all its adjacent nodes is initially assumed.



Figure 1. Electric grid embedded on the geometry. Two adjacent bundles are shown. Transparency is used to enhance visualization.

The creation of base models consists of the following five steps (illustrated in Figures 1-3). It is only step A1 that requires intense user interaction:

A1. *Manual segmentation into a hierarchy of muscle*

bundles. Following histology data [1], groups of basic elements are selected using their connectivity to neighboring elements; the depth of selection is controlled by the user. A “seed” is manually selected and it “propagates” to its neighbors. A number of additional features are implemented to facilitate this process, such as surface rendering, transparency, superimposing already segmented geometry, etc.

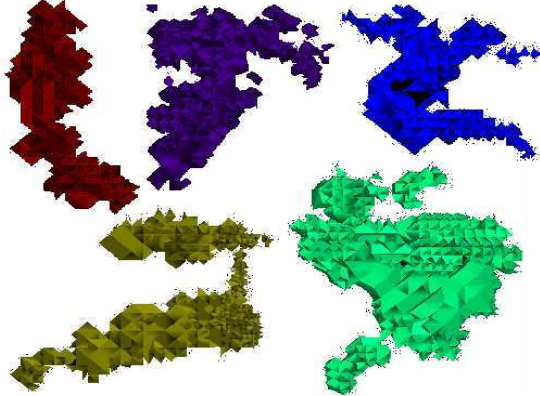


Figure 2. Some of the bundles produced. From top-left to right bottom: Crista Terminalis, left auricle: anterior superficial and deep bundles, analogously for posterior

A2. *Subdivision of bundles into domains*. Since inter-bundle connectivity is not homogeneous along the bundle [1], three domains per bundle can be specified; this is achieved by specifying a percentage of the bundle to each. The center of mass for the bundle is the reference.

A3. *Inter-bundle connectivity in a per-domain vs. per-connecting-bundle basis*; thus, reducing connectivity between bundles. This is specified as a percentage of Gap Junctions (GJ) that should not be removed from the initial basis “all elements are interconnected to all immediate neighboring elements by GJ”.

A4. *Assign Fiber Orientation (FO)*. This is applied to each bundle, by choosing sets of control points, one set a time, which dictates FO for a subset of elements of a bundle; this allows specifying complex FOs. Each control set specified is used to create a curve following the Chaikin algorithm [6], iterated until every line segment has a length less or equal to the averaged myocyte length. A pair of consecutive points in the curve defines two parallel planes (at least within a sufficiently long distance); their normal defined by the direction vector towards the other point. The volume in between these planes and the distance between the original user-defined control points, delineate the elements that should be assigned this FO (plane’s normal). Elements that fall in a second volume have their FO affected by a weighting equation in function of the element’s volume that belongs to each control volume.

A5. *Heterogeneities and discontinuity within bundles*.

Heterogeneities are introduced as described in [7], using random noise maps, although they have the disadvantage of not being fully reproducible. Discontinuities on the other hand are created by means of defining tissue “layers” (identified in [8]), represented as surfaces, in the direction of the FO.

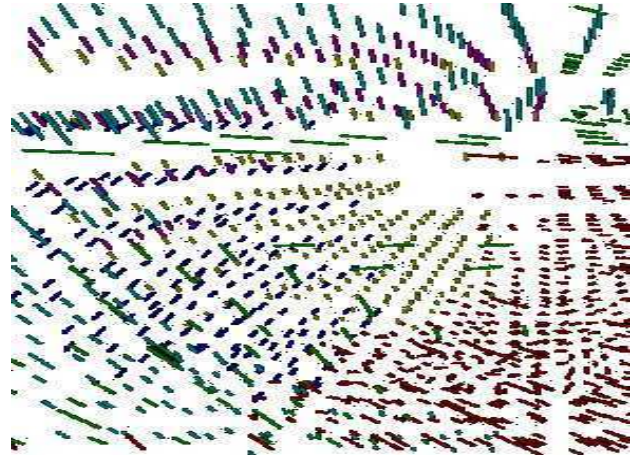


Figure 3. FO is assigned not only per bundle but by region on a bundle. Lines of the same color represent FO for a bundle; note that there are variations within bundles

Because of the flexibility of the Finite Volume Method regarding mesh requirements [7], and the likely complexity of the meshes, the output mesh is intended to be used with it. Parameters like Ion concentration, resting potential, conductivity, etc, can be easily modified in a per-bundle basis.

The semiautomatic process uses a base model (result of the steps above) to produce a new model representing a new base model and/or a patient specific one. Here, the work required to complete step B1, is greatly alleviated in comparison to A1.

B1. The new mesh must be trimmed from non-atrial geometry in order for the base model to optimally register. To fit the base model to the new mesh, the former is warped using a surface detection algorithm and sample control points. For registration, the models are aligned first in relation to their centers of mass, then, orientation (pitch, yaw and roll) must be manually approximated so the automatic process completes successfully.

B2. An axial representation per bundle of the original model is retrieved; a curve running along the relative center of mass and in the direction of the bundle’s FO.

B3. For each bundle axis curve, a relationship to the other curves is found in terms of distance between end points and atrial center of mass. Control points for user manipulation are defined to enhance model registration between the base model and the new mesh, thus accounting for slight anatomy variations. The

aforementioned distances can be slightly scaled up/or down as required.

B4. Once fitted, the new bundles are created by including all the elements that are contained within the limits of the surface defined by the base model bundle. In addition, FO is mapped to the new elements; every new element will acquire the FO of the base element if the distance between centroids is under half the average myocyte length of the new model's bundle.

B5. Although other parameters are assigned altogether with FO, these are processed and applied separately as during A5 (i.e. connectivity, domain subdivision, heterogeneities, etc). The resulting model can be manually refined at any stage of the process. For example, any anatomy left out of any bundle during B4 can be easily visualized by rendering semi-transparent bundle surfaces. Further fine tuning of the model should ideally result from visual inspection of sample MRI or CT slices taken from the new patient.

3. Results

To test the software and the algorithms, two different scenarios were prepared. For the initial test, a mathematically generated semi-structured hexahedral mesh of a hollow sphere with a thickness was used. The target mesh used was equal but using elements of $\frac{3}{4}$ of the original size. For the second scenario, real heart meshes were used. A base model was created using an adaptive and unstructured tetrahedral mesh. The target mesh for semiautomatic processing was one of a higher resolution and different topology; a non-adaptive, structured tetrahedral mesh.

Manual segmentation into bundles for the heart mesh required 21 man hours; this was carried out by two medical students. The process included a steep learning curve, although they recognized that a subsequent process should take considerably less time. Only 14 muscle bundles (structures) were defined because time available was limited, the bundles being: (1) Terminal Crest, (2&3) two thin epicardial layers of the Inter-Atrial Bands, one superior and one anterior, (4,5,6&7) for the left auricle anterior and posterior bands at two levels of depth (epi to mid myocardium and mid to endocardium), (8) and a lateral bundle including all the thickness of the wall, (9&10) analogously for the right atrium but only from anterior, (11) a bundle for the superior of about half the wall in thickness, (12) whereas posterior was left as "bulk" tissue including all the thickness of the wall, (13&14) Mitral and Tricuspid valves' Annulus. Other structures like the Pectinate muscles were not created. Features like the tissue inserting into the pulmonary veins was not considered (veins were completely removed).

"Painting" the FO required less than 5 hours; the level of detail for this was not thoroughly observed.

Nevertheless, it is uncomplicated to refine the specification for FO, whereas it is much more costly to refine bundle segmentation.

The automatic process takes only a few minutes. Model refinement may take several hours depending on the needs and how suitable was the base model to fit into the new (i.e. similarity of heart's anatomy). The quality of the results varied significantly depending on the manual input from the user regarding registration of model orientation and scaling.

The resulting output model includes features useful for simulation such as "severing" gap junctions, altering myocyte functionality, control of local and regional model properties. The potential is on hand for creating special bundles: e.g. conduction or isolation paths, or a SAN bundle, and parameterization of their biological behavior/status.

The model itself provides a data structure (storage and retrieval) for each element to support biophysical simulations for the Monodomain model (simulation data). The electric grid embedded responds to "queries" regarding propagation to neighboring elements (where to be propagated and corresponding resistivity).

Finally, a characteristic not originally intended but discovered is that of readiness for tissue contraction. Given that every element has its FO vector, by establishing a relationship between change in membrane potential and contraction, the whole model contracts in a complex manner (which including twisting). After specifying regions (parts of bundles) attached to a heart skeleton, these "rule" the contraction of the other elements towards them. A simple scaling factor to test this was used: elements "pull" their vertexes in a parallel direction towards its centroid at a rate of $\text{ElementLength}/95\text{mV}$. Initial experiments regarding this are already in course.

4. Discussion and conclusions

The model is designed for FV solvers for the Monodomain approach. Support for Bi-domain implies a few but important changes; on the other hand, support for another method like Fine Differences may be more complicated and has not been thoroughly studied.

Qualitatively, the results from the automatic process are more than acceptable and show a fair correlation. At the moment, this evaluation is by visual inspection only, but it was possible to identify a fairly good match of the surfaces both on the epicardium and endocardium; nevertheless, there are some mismatches following deformation after a few layers of elements, particularly those connecting to other bundles.

During model generation, intermediate stages can be saved, retrieved and edited to alter the resulting model; thus providing flexible resources for experimentation.

The algorithm was tested both on structured and unstructured meshes; although the only hexahedral mesh available was mathematically defined. Cross-topology compatibility is not ideal, i.e. structured vs. unstructured. Nevertheless, more experiments need to be made using more target models and a better base model.

The modeling process used aims to leave behind the Cardiac Syncytium paradigm without having to alter the current mathematical formulations. As described by [8], this is a factor that must be taken more seriously for the future of simulations.

This is an ongoing project; a number of enhancements and fine-tuning of the algorithms are planned, namely:

A refinement of the warping algorithms and a more detailed segmented base model; new models can only be as accurate as the base model used. In addition, a technique to minimize energy during deformation is being investigated [9].

Using meshes of different resolution (both in number of elements and coming from different MRI resolutions), test how they behave for both this process and biophysical simulations; particularly the resolution tolerance for the models proposed here.

Curve fitting for FO is currently done using a modified Chaikins approach. Although elegant and very simple to implement, it curves too soon and “shrinks” away from the end points. We shall try Bernstein polynomials.

Ideally, target-model registration should be in a semi-automatic feedback loop using sample MRI slices. In addition, FO could be at least partially loaded from DTMRI datasets. FO for patient-specific models should preferably be adjusted or compared to sample slices of DTMRI datasets.

To prove the worthiness of the models proposed, biophysical simulations following a well defined set of experimentation scenarios are required. These should include the impact of changing model parameters and resolutions as compared to conventional full 3D or Monolayer models; ultimately, running comparisons between real and virtual ECGs from patient-specific models during sinus rhythm. Moreover, it would be interesting to investigate quantitative effects of using structured vs. unstructured meshes.

The model is ready to act as a plug-in geometry for a compatible FV solver. Perhaps either an interface will be required, or given its flexibility, it may just be adjusted.

On the long term, and as research moves to provide better approximations to the “Inverse Problem” solution, the ultimate goal is to produce ECG-modulated biophysical models.

The software was built using C++, Open GL & WinForms (for GUI). An added value is the design, documentation, and coding of the software; good practices for systems engineering were employed such as

using UML and OOD.

Acknowledgements

Thanks to Hector Ibarra and Blanca Vallejo (Facultad de Medicina, UANL, Monterrey Mexico) for kindly segmenting the base model into bundles, and to Dr. Robert Anderson, MD, (London Imperial, retired) for his guidance regarding Atrial Architecture.

Initial heart meshes were provided by the CVC at The University of Texas at Austin, USA (unstructured), and by Dr. Daniel Einstein from Pacific Northwest National Laboratory, Washington, USA (structured).

Special thanks to Professor Roger Phillips from Hull University for revising this article, and to CONACYT, Mexico, for funding my PhD.

References

- [1] Ho SY, Anderson RH, Sánchez-Quintana D. Atrial Structure and Fibres: Morphologic bases of Atrial Conduction. *Card. Research*, 2002; 54: 325-336
- [2] Harrild DM, Henriquez CS. A Computer Model of Normal Conduction in the Human Atria. *Circulation Research* 2000; 87: 25-36
- [3] Kuijpers NHL, Eikelder HMM, Prinzen FW. Adaptive Modeling of Ionic Membrane Currents Improves Models of Cardiac Electromechanics. *Proceedings of Computers in Cardiology 2008; Bologna Italy*, In Press.
- [4] Kurata Y, Hisatome I, Imanishi S, Shibamoto T. Dynamical Description of Sinoatrial Node Pacemaking: Improved Mathematical Model for Primary Pacemaker Cell. *Am. J. Physiol. Heart Circ. Physiol.* 2002; 283, 5: 2074-2101
- [5] Stewart P, Aslanidi OV, Zhang H. A Novel Mathematical Model of the Electrical AP in a Canine Purkinje Fiber Cell. *Computers in Cardiology 2007*; 34: 363-366
- [6] Chaikin G., An algorithm for High Speed Curve Generation, *Computer Graphics and Image Processing*, 1974, pp 346-349
- [7] Jacquemet V., A Biophysical Model of Atrial Fibrillation and Electrograms: Formulation, Validation and Applications, PhD Thesis, École Polytechnique Fédérale de Lausanne, 2004
- [8] Trew M., Legrice I., Smaill, B., Pullan A., A Finite Volume Method for Modeling Discontinuous Electrical Activation in Cardiac Tissue, *Annals of Biomedical Engineering*, 2005, Vol. 33, No. 5, pp 590-602
- [9] Bookstein FL. Principal Warps: Thin-Plate Splines and the Decomposition of Deformations. *IEEE Trans. On Pattern Analysis and Machine Intelligence* 1989; 11, 6: 567-585

Address for correspondence

Bernardo D. Flores Hermosillo, MSc
SimViz Group, Department of Computer Sciences
Hull University, Cottingham Road, HU67RX
United Kingdom
b.flores-hermosillo@dcs.hull.ac.uk